sustainability

MDPI

Article

Improved Granite Residual Soils from a Study on Diesel Contamination in East Hunan Province

Qiunan Chen [1], Kun Long [2], Xiaocheng Huang [2,*], Zhenghong Chen [2] and Yongchao He [3]

[1] Hunan Province Key Laboratory of Geotechnical Engineering for Stability Control and Health Monitoring, Hunan University of Science and Technology, Xiangtan 411201, China
[2] School of Civil Engineering, Hunan University of Science and Technology, Xiangtan 411201, China
[3] College of Resource & Environment and Safety Engineering, Hunan University of Science and Technology, Xiangtan 411201, China
* Correspondence: xiaochenghuang@163.com

Abstract: Soil can be amended with cement, lime, fly ash and other curing agents after diesel contamination. In this study, a diesel-contaminated granite residual soil with an oil content of 9% was selected and amended with cement, lime and fly ash as curing agents and their incorporation levels were varied. A straight shear test showed that 6% lime resulted in the best improvement in the contaminated soil, with a cohesive force of 122.1 kPa and an internal friction angle of 27.1°. A disintegration test revealed that the disintegration resistance of the contaminated soil was improved by 6% cement, 20% fly ash and 10% lime, with 10% lime being the most effective. SEM tests revealed that diesel fuel acted as a constant pore fluid to cause significant fragmentation and separation of the granite residual soil from flakes and blocks to smaller agglomerates and fragments. The curing agent, by increasing the physical reaction products, causes the particles to agglomerate, filling the soil pores and enhancing the integrity of the soil, thus improving the soil properties.

Keywords: diesel-contaminated soils; granite residual soils; curing agent amendment; straight shear; disintegration; microstructure

check for updates

Citation: Chen, Q.; Long, K.; Huang, X.; Chen, Z.; He, Y. Improved Granite Residual Soils from a Study on Diesel Contamination in East Hunan Province. *Sustainability* **2023**, *15*, 4900. https://doi.org/10.3390/su15064900

Academic Editors: Jun Hu, Guan Chen and Yong Fu

Received: 5 February 2023
Revised: 25 February 2023
Accepted: 27 February 2023
Published: 9 March 2023

1. Introduction

During the operation of large diesel engines, pollution problems can occur, such as ruptured oil pipelines, leaking storage tanks and overturned construction vehicles [1–4]. These accidents can cause damage to the surrounding soil and the ecological environment, reducing the soil's resistance to scouring, stability and load-bearing capacity [5], and making it susceptible to landslides and depressions when contaminated with diesel. Therefore, it is vital to treat contaminated soils, and treatment methods generally fall into three categories: physical, chemical and biological [6,7]. Physical methods [8,9] aim to prevent the migration and spread of contaminants through the physical layer and maintain the basic properties of the original soil, whereas chemical treatment methods [10,11] rely on oxidation–reduction and other chemical reactions to eliminate the effects of contaminants. Although effective, biological treatment methods [12,13] are often costly and complex to operate since they use microorganisms or plants to absorb contaminants. Treatment with a curing agent [14,15], which is a combination of physical and chemical treatment methods, is a low-cost and straightforward treatment option. In regions such as Xiangdong in Hunan, central Fujian, Western Guangdong, and other provinces where granite residues are widely distributed [16,17], granite residues have become the main contaminant of diesel and its derivatives, and therefore curing agents become an important treatment option to prevent the unimaginable consequences of contamination.

In engineering, many studies have been conducted on the treatment of petroleum-contaminated soils. In 2003, Shah et al. [18] conducted an experimental study on petrol-contaminated clay soils, which found that petrol contamination significantly affected the engineering properties of soils. Cement, lime and fly ash were found to have ameliorative effects on the stability of clay-contaminated soils, providing valuable guidance for the treatment of petroleum-contaminated soils. Zheng et al. [19] investigated changes in the dry density and compaction curves of soil samples contaminated by varying degrees of diesel fuel and with different pore fluids through indoor tests. Khosravi et al. [20] investigated diesel-contaminated kaolin, while He et al. [21] investigated the basic engineering properties and microstructural changes in diesel-contaminated soils in the Changchun area before and after cement modification through a series of indoor tests. They analysed in great depth the way in which cement curing agents affect soil properties. Li et al. [22] investigated the effect of di-cement soil on the curing of coastal saline soils by controlling the temperature and optimising the design, taking into account the climatic conditions in the area, for the treatment of oil-contaminated soils in coastal areas. Li et al. [23] studied the effect of cement mortar on diesel-contaminated soils, using the Sichuan–Tibet Railway construction project as a practical basis, and found that the cement mortar was effective in curing diesel-contaminated soil. These studies have made important contributions to the treatment of petroleum-contaminated soil in engineering practice and provide valuable guidance for future research in this area.

Granite residual soils are known to have poor soil homogeneity and are prone to disintegrate in the presence of water, which exacerbates soil instability when exposed to petroleum and its derivatives, resulting in challenging land contamination issues. Zhang et al. [24] conducted disintegration tests under different conditions to identify the disintegration mechanisms and influencing factors of granite residual soils in Guangzhou. Zhao et al. [25] improved granite residual soil in the Nanyue area by selecting an admixture of cement, lime and fibre to improve the granite residual soil, and then studied the effect of the three improvers through triaxial tests and disintegration tests; they found that the properties of the soil were changed in differing degrees after the addition of the three different types of materials. Wang et al. [26] investigated the mechanical properties of granite residual soil samples collected in Rongxian, Guangxi, using various tests and analysed their microstructure. For granite residual accumulated soil in Buji, Singapore, Zhang et al. [27] obtained relevant physical and mechanical parameters and studied their engineering properties. Tang et al. [28] studied the disintegration mechanism of modified granite residual soils under dry and wet cycles in South China. These studies offer valuable insights into the disintegration and engineering properties of granite residual soils, which can guide the treatment of petroleum-contaminated soils and improve soil stability in various regions. Through these studies, we have found that the gel particles produced by cement hydration can fill soil pores, reduce soil compressibility and improve overall strength, while weakening the lubricating effect of diesel fuel, enabling soil particles to form larger clumps and enhancing soil integrity. Fly ash can modify porosity, improve air permeability and water-holding capacity, fill larger pores of sandy soils with tiny particles, modify the distribution of soil pores, regulate soil infiltration characteristics and prevent soil erosion. Lime amendments, on the other hand, generate a lot of heat by reacting with water to produce calcium hydroxide, which helps to remove contaminants.

In this paper, cement, fly ash and lime were used as curing agents to investigate their effectiveness in improving the performance of diesel-contaminated granite residual soils in the east of Xiangtan. By combining the existing literature and the group's research, direct shear tests, disintegration tests and scanning electron microscopy tests were conducted on diesel-contaminated granite residual soil with an oil content of 9%. This study demonstrates that cement, lime and fly ash can improve the mechanical properties of diesel-contaminated granite residual soils to varying degrees, making the soil more resistant to disintegration and better able to meet engineering requirements. Additionally, it explains the principle of contaminated soil improvement after curing agent treatment from a microscopic perspective. By selecting the appropriate curing agent and ratio, soil pollution treatment can be achieved effectively, while also using resources efficiently and reducing costs. Research on curing agent treatment technology can promote its practical application in engineering and provide feasible technical solutions for soil pollution treatment.

2. Materials and Methods

2.1. Soil Samples

The original soil sample was taken from a newly excavated slope located adjacent to the national highway in Miaoling Town, Zhuzhou City, Hunan Province. The sample was excavated at a depth of 1.2 m in the middle of the slope (Figure 1). After a series of indoor geotechnical tests, the physical characteristics of the original soil sample are presented in Table 1, while the particle size distribution is illustrated in Figure 2. To contaminate the test soil sample, 0# diesel oil, which is sold by a petroleum company in Xiangtan, Hunan, Sinopec, was chosen. The diesel oil has a relative density of 0.841 g/cm^{-3}, and appears as a light yellow, slightly lustrous liquid that is slightly soluble in water. It is less viscous than crude oil but more viscous than water. The diesel oil has a strong volatility and an irritating odour when exposed to air.

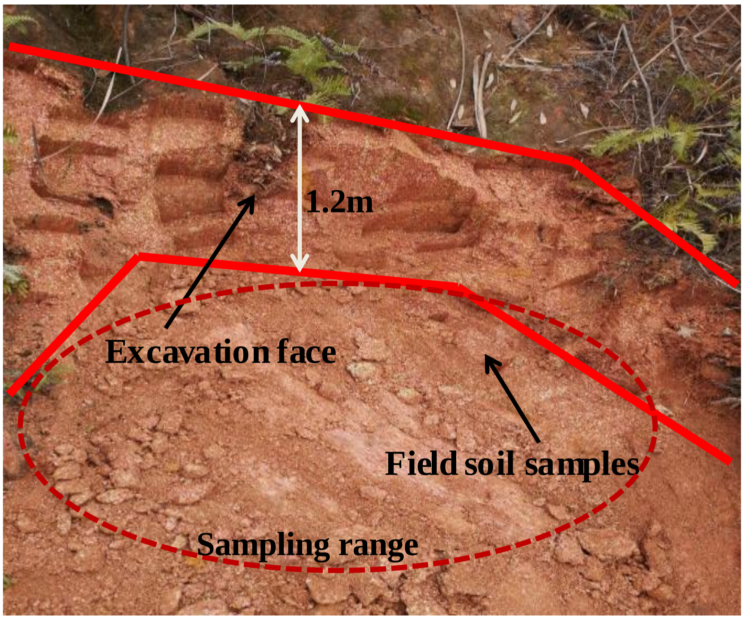

Figure 1. Excavation slope of granite residual soil.

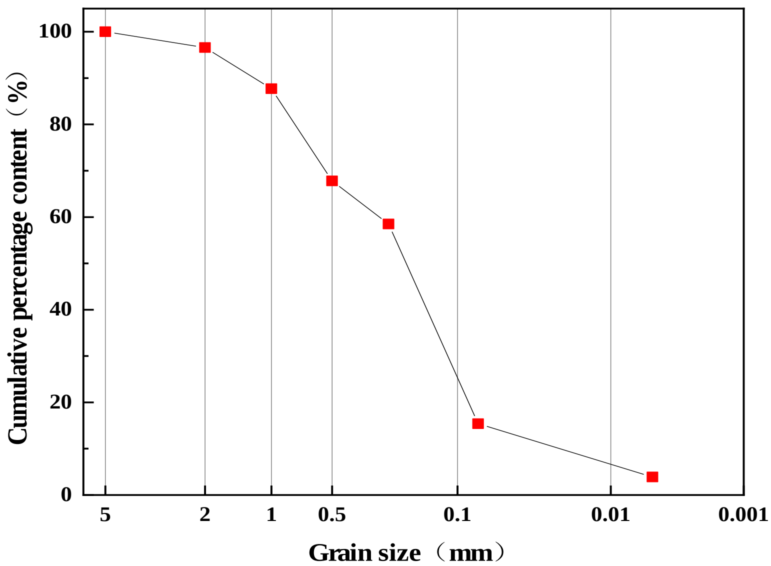

Figure 2. Particle gradation curve of soil sample.

Table 1. Physical indicators of in situ soil samples.

Soil Sample	Water Content of W (%)	Density G_s (g/cm^3)	Cohesion C (kPa)	Internal Friction Angleφ (°)	Liquid Limit W_L(%)	Plastic Limit W_P(%)	Plasticity Index I_P
undisturbed soil	22.7	2.67	25.46	35.7	37.1	26.1	11.0

2.2. Diesel-Contaminated Soil Samples

Soil samples were prepared by uniformly spraying different levels of diesel fuel (mass ratio of diesel fuel to air-dried soil sample) with 0%, 3%, 6%, 9%, 12% and 15% oil content of diesel-fuel-contaminated modified granite residual soil. The soil samples were then sprayed with the calculated weight of pure water, turned over, stirred well, and placed in sealed bags and left to stand for 24h (Figure 3). All specimens were left for one week to allow the mixture of organic chemicals and soil to equilibrate and to ensure that the pore fluid concentrations in the soil samples remained consistent [29,30]. The contaminated soil samples were later subjected to compaction tests, straight shear tests and consistency threshold tests to derive their engineering properties' parameters. From Table 2, it can be seen that the diesel-contaminated granite residual soil with 9% oil content was weakened the most and all parameters decreased the most, so the contaminated soil with 9% oil content was chosen as the object of study.

(**a**)

(**b**)

Figure 3. Preparation of diesel-oil-contaminated granite residual soil. (**a**) Soil sample after addition of diesel; (**b**) Sealing of contaminated soil.

Table 2. Parameters of soil samples with different oil content.

Soil Oil Content (%)	Cohesion C (kPa)	Internal Friction Angle φ (°)	Liquid Limit W_L (%)	Plastic Limit W_P (%)	Plasticity Index I_P	Optimum Moisture Content W (%)
3	22.15	31.6	36.1	24.4	11.8	14.5
6	22.96	29.0	33.2	19.2	14.0	11.75
9	21.60	25.1	30.7	18.0	12.7	11.31
12	22.01	25.5	29.3	17.3	12.0	7.14
15	26.65	26.7	29.6	17.6	12.0	7.04

2.3. Test Method

The tests to improve soils contaminated with 9% oil content were mainly conducted through direct shear tests, disintegration tests [31,32] and scanning electron microscopy tests. The direct shear test is used to determine the soil's shear strength by applying shear stress to the soil sample, while the disintegration test is used to study the soil's stability and durability by saturating the soil sample with water. The scanning electron microscopy test can be used to observe the soil's microstructure, pore distribution and shape, grain size composition, and more. The results of these three tests can be corroborated to provide structural information that is essential in interpreting the soil's mechanical properties.

The direct shear test [33] is conducted using an electric strain gauge, as depicted in Figure 4. Initially, the upper and lower boxes of the shear container are aligned, followed by the insertion of the fixing pin as well as the placement of the permeable stone and filter paper in the lower box. Then, the ring knife blade is aligned with the specimen, and the filter paper and permeable stone are placed on top of the specimen. Next, the specimen is carefully pushed into the shear box. The drive is then moved so that the steel ball at the front of the upper box is in contact with the force gauge, and the pressure transfer plate and pressure frame are added sequentially. The vertical displacement measuring device is installed, and the initial reading is taken. The soil sample is then subjected to vertical pressures of 100 kPa, 200 kPa, 300 kPa and 400 kPa, and the fixing pin is removed. The fast shear test is conducted at a shear rate of 0.8 mm/min, and the force gauge reading is recorded at regular intervals until shear failure occurs.

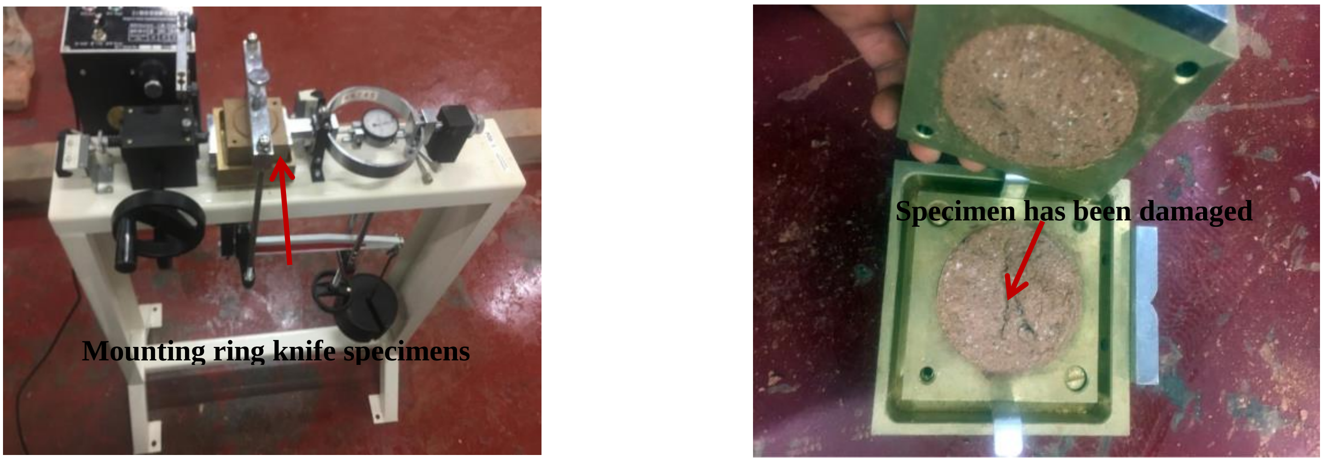

(**a**) (**b**)

Figure 4. Direct shear test: (**a**) test instruments; (**b**) soil samples are damaged.

The disintegration test apparatus comprises a transparent glass sink, a metal mesh basket, a force transducer, a fixing hook, a digital display and a computer. The soil sample used for the test is cylindrical, 7.6 cm high, and 3.91 cm in diameter (Figure 5). As the water content can significantly affect the disintegration test results, the water content of the test soil sample is uniformly controlled to around 15% to control the impact of moisture on the oil content within the sample. Before starting the test, an appropriate amount of pure water is added to the glass box, so that the basket is immersed in water about 10 cm below the surface. Then, the mobile phone camera, fixed to the side, is turned on, and the computer software is opened to record the test. The specimen is then slowly placed in the basket, and the disintegration process is initiated.

The disintegration test typically describes the disintegration characteristics of soil by comparing the rate of disintegration. The formula for calculating the disintegration rate H is as follows:

$$H = \frac{M_{\max} - M_{\text{disintegration}}}{M_{\max}} \times axin \quad (1)$$

H is the disintegration rate, $M_{\text{disintegration}}$ is the mass of the soil sample lost by disintegration at a certain moment and $M_{\max}$ is the mass of the soil sample stabilised by water absorption and saturation.

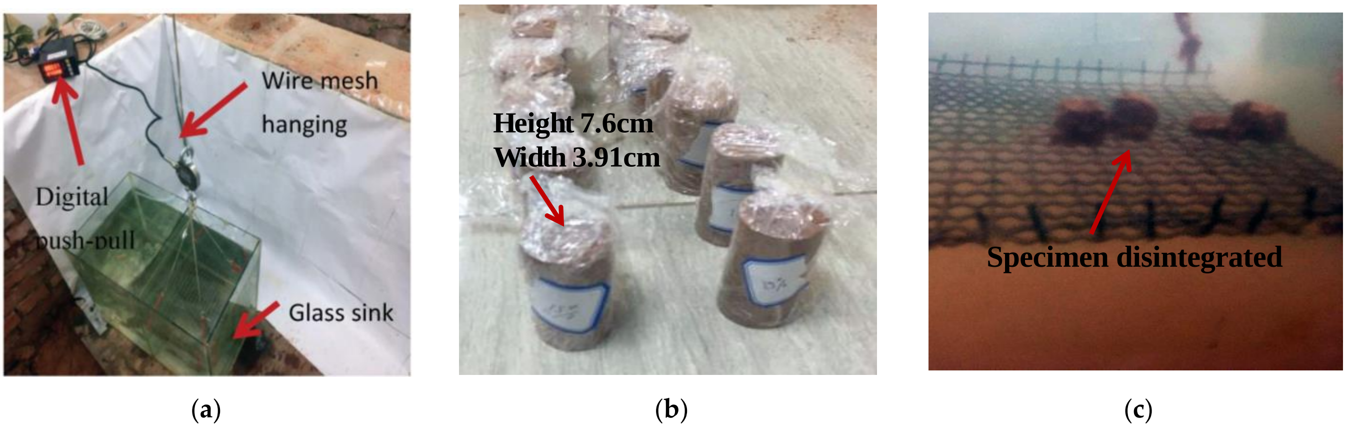

Figure 5. Conducting the disintegration test: (**a**) test equipment; (**b**) disintegration test soil samples; (**c**) soil sample disintegration is complete.

Finally, the SEM electron microscope scanning test was carried out in conjunction with the test apparatus shown in Figure 6 below. The soil sample was ground into fine particles and then coated with gold to increase its electrical conductivity for subsequent observation. The prepared sample was then placed on the SEM sample stage and fixed in place. A magnification of 2000× was selected and the surface of the sample was scanned using the electron beam. The image was observed and the position and focus of the sample were adjusted to ensure that the surface of the sample was clearly visible. The morphology and structure of the sample surface were then observed, looking for distinctive features to photograph, and finally, the image was saved. By examining the microstructure of the soil samples, it was possible to analyse the mechanism by which the soil was weakened by diesel fuel with varying oil content and the mechanism by which different curing agents ameliorated diesel pollution.

Figure 6. Electron microscope scanning tests were performed: (**a**) testing instruments; (**b**) test samples.

3. Results and Discussion

3.1. Direct Shear Test Results

For the diesel-contaminated granite residual soil with 9% oil content, different levels of curing agents were mixed before conducting the direct shear tests to measure the corresponding shear stress changes. The results are illustrated in Figure 7.

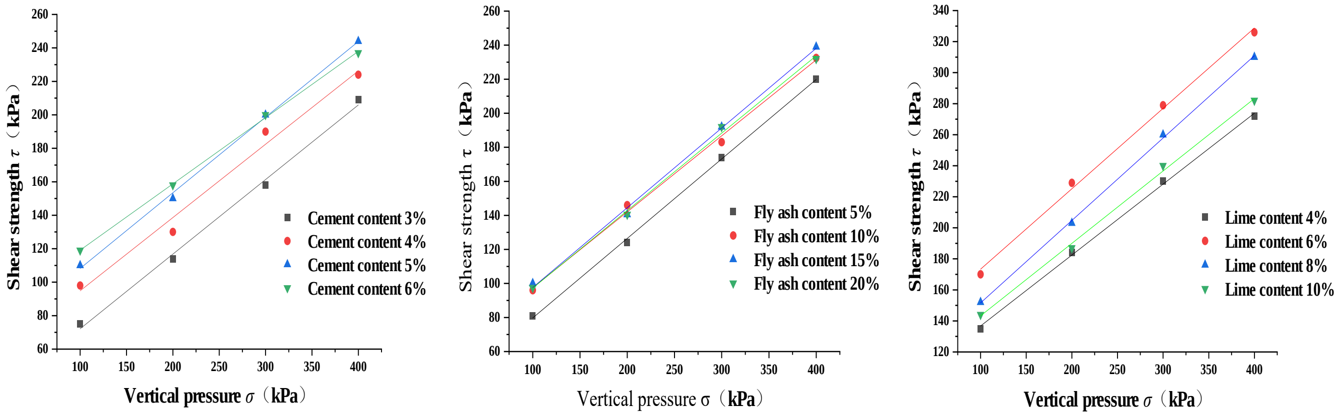

(**a**) (**b**) (**c**)

Figure 7. Variation law of shear strength of modified soil under direct shear test: (**a**) different cement blending amount; (**b**) different fly ash blending amount; (**c**) different lime blending amount.

In Figure 7, (a) indicates that the shear strength of the 9% diesel-contaminated granite residual soil mixed with 6% cement admixture is the highest at 122.1 kPa when subjected to a vertical pressure of 100 kPa. However, as the vertical pressure increases, the shear strength of the 5% cement admixture gradually exceeds that of the 6% cement admixture and reaches the highest level. In (b), under the initial vertical pressure, the shear strength of the 5% fly ash admixture is lower than that of the other fly ash admixtures. As the vertical pressure increases, the shear strength of the 15% fly ash admixture increases and ultimately becomes the highest. At the same vertical pressure, the oil-stained soil mixed with 6% lime has the highest shear strength and the best improvement. Table 3 shows the shear strength values of the improved soils with the three admixtures.

Table 3. The shear strength index of the modified soil under different curing agents.

The Curing Agent Mixing Dosage (%)	Oil-Contaminated Soil Cohesive Force C (kPa)	Internal Friction Angle of Oil Soil φ (°)
5% Cement admixture	77.5	22.0
15% Fly ash admixture	57.3	24.3
6% Lime admixture	122.1	27.1

3.2. Results of the Disintegration Test

Figure 8 displays the disintegration curves of the residual diesel-contaminated granite soils mixed with various concentrations of different curing agents during disintegration testing:

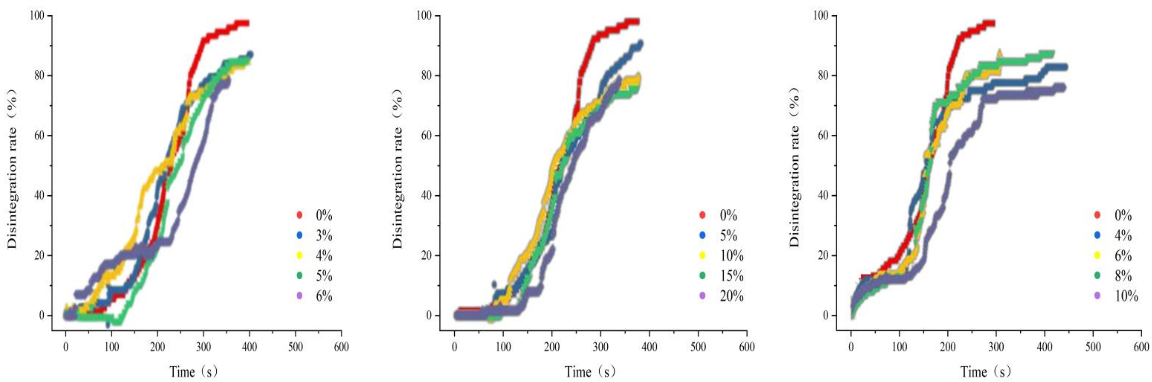

(**a**) (**b**) (**c**)

Figure 8. Disassembly curve of the improved soil under the disintegration test: (**a**) different cement blending amount; (**b**) different fly ash blending amount; (**c**) different lime blending amount.

The average disintegration rate of section *AB* was used to compare the disintegration rates of soils with different oil contents, and the disintegration rate *V* was calculated using the following equation:

$$V = \frac{H_B - H_A}{T_B - T_A} \quad (2)$$

V stands for average disintegration rate, H_A and H_B for soil sample disintegration rates at places *A* and *B*, and T_A and T_B for instantaneous timing at the same locations. This allows one to determine the corresponding disintegration rates, as seen in Figure 9 below:

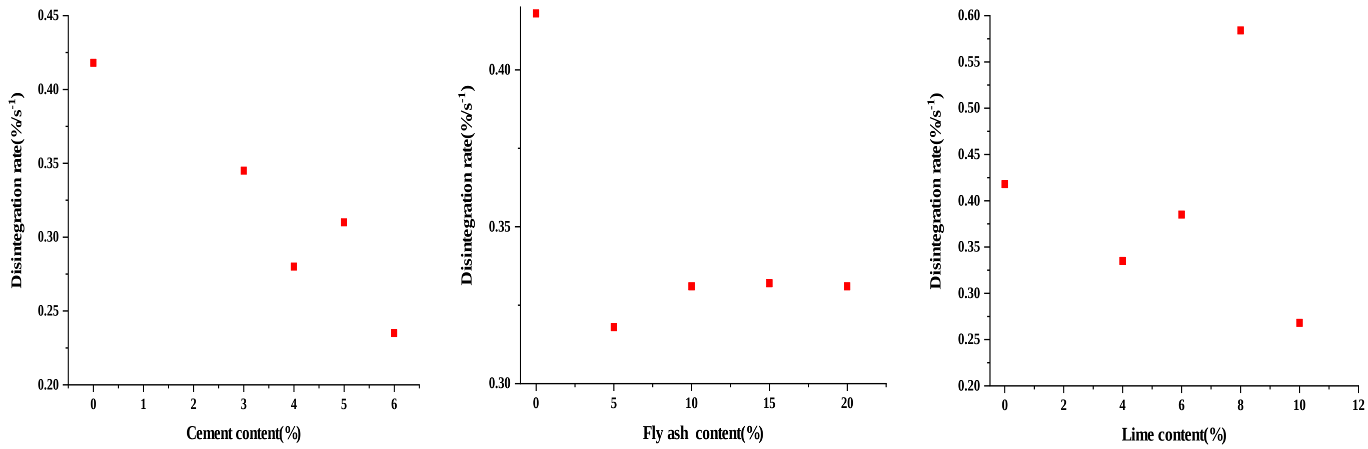

(**a**) (**b**) (**c**)

Figure 9. Disassembly rate of oil-contaminated soil under different mixing amounts of different curing agents: (**a**) different cement content; (**b**) different fly ash content; and (**c**) different lime content.

In terms of improvement, Figure 8a shows that the sample with 6% cement performed better than all the other specimens. The disintegration rate curve of this specimen was the smoothest, and the disintegration rate was the smallest. Although the disintegration occurred the earliest, the amount of disintegration was small, and the specimen remained intact with no disintegration occurring at the joints of the soil layers. The analysis suggests that the earliest disintegration occurred because a high amount of curing agent was incorporated, resulting in a reduction in water between the soil particles within the specimen. Although the hydration reaction was effective, it affected the specimen's integrity to some extent. Observing Figure 9a, it can be seen that the rate of disintegration of specimens generally tends to decrease as the amount of cement is increased. This means that the incorporation of cement as a curing agent slows down the disintegration of the soil sample and strengthens its integrity to a certain extent.

According to Figure 8b, the highest resistance to disintegration was found in the 20% fly ash admixture, which had the smoothest disintegration rate curve and the lowest disintegration rate, with disintegration occurring the latest. As shown in Figure 9b, the disintegration rates of the specimens decreased after the addition of the fly ash admixture. However, the disintegration rate of the specimens did not decrease further as the amount of admixture continued to increase. Our analysis suggests that the amelioration mechanism of fly ash is different from that of cement and lime, which resulted in no reduction in the disintegration rate. The amelioration mechanism of fly ash is changing the distribution of soil pore space by filling the larger pores of sandy soils with its fine particles to improve the water-holding capacity of the soil. This is different from the chemical reaction of cement and lime that achieves soil flocculation and gelation.

After comparing (a), (b), and (c) in Figure 8, it is evident that lime has the most effective results of the three curing agents in enhancing the disintegration resistance of diesel-contaminated granite residual soil. In contrast to the other two curing agents, lime blended specimens displayed more significant changes in mass during the water absorption saturation phase, which resulted from the secondary reaction between the lime and water in the test chamber when the sample was not completely reacted with the soil. The sample with 10% lime blending exhibited the strongest disintegration resistance, with the smoothest disintegration rate curve and the lowest disintegration rate. In contrast, the disintegration rate of 9% diesel-contaminated granite residual soil varied unevenly, which is related to the degree of completion of lime hydration reaction during the sample preparation.

3.3. SEM Test Results

A direct shear test and a disintegration test were performed to determine the optimal dosage of curing agents. The results indicated that a dosage of 5% cement, 15% fly ash and 6% lime had the best improvement. These three dosages were selected for electron microscope scanning tests. The soil sample parameters scanned by each SEM group are listed in Table 4 below:

Table 4. Grouping of EM scanning tests.

Sample Name	Oil Length (%)	Cement Curing Agent The Amount of Incorporation Was (%)	Fly Ash Curing Agent The Amount of Incorporation Was (%)	Lime Curing Agent The Amount of Incorporation Was (%)
Y1	0	0	0	0
Y2	6	0	0	0
Y3	12	0	0	0
Y4	0	5	0	0
Y5	6	5	0	0
Y6	12	5	0	0
Y7	0	0	15	0
Y8	6	0	15	0
Y9	12	0	15	0
Y10	0	0	0	6
Y11	6	0	0	6
Y12	12	0	0	6

Y1–Y3 are unamended oil-contaminated soil specimens with different oil contents (0%, 6% and 12% in that order), which were scanned separately by SEM electron microscopy, resulting in the following microstructure diagrams.

The geotechnical properties of soil are influenced by their structure, which is the arrangement of mineral particles in a structural framework [34]. During deposition, clay particles tend to attract each other and form flocculated structures when attracted by external forces, while they tend to move and form dispersed structures when repelled by external forces. Therefore, changes in the pore fluid affect the soil structure. Figure 10 displays SEM micrographs of diesel-contaminated granite residual soils with oil contents of 0%, 6% and 12%. In Y1, the granite residual soil particles can be observed to be large in volume and distributed in sheets with moderate soil pore space. In Figure 10(Y2,Y3), an increase in the number of finer soil particles can be observed, and the diesel-contaminated granite residual soil undergoes significant fragmentation and separation, changing from a flaky, lumpy structure to smaller particle sizes of agglomerates and fragments. In particular, the pore size of the soil samples became larger when the oil content was 12%. When soil particles are contaminated with diesel oil, a layer of contaminants surrounds them and does not allow their interaction with each other. The contaminated soil particles act individually, and they tend to behave similarly to silt particles. As a result, the structure of the soil will be looser in the presence of diesel fuel, and the granite residual soil will be more prone to disintegration. In addition, the diesel acts as a lubricant between the individual particles, and they can slide more easily against each other. As a result, the shear strength of the granite soil residue will be reduced in the presence of diesel molecules. Soil particles with diesel fuel attached cannot absorb water molecules, and they can expel more water, which further affects the consistency limits and infiltration properties of the soil. This shows that the presence of diesel fuel has a significant effect on soil structure and properties.

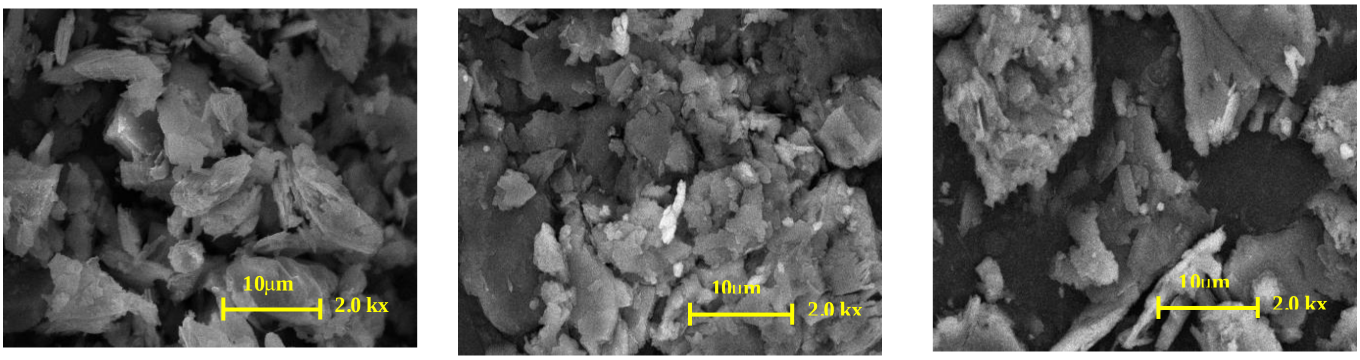

Y1 Y2 Y3

Figure 10. SEM microstructure of soil sample without curing agent.

The microstructure for the modified soil specimens Y4–Y12 mixed with different levels of curing agent is shown below:

Upon comparing Y1–Y3 with Y4–Y12, it is evident that the addition of the curing agent significantly reduces the soil sample's fragmentation and forms a blocky and agglomerated structure, which carries flocculent branches. When examining specimens amended with the same curing agent at different oil contents, it is observed that cement-amended granite residual soil specimens have significantly reduced pores, and the cement hydration products bind fine soil particles and improve the integrity of the soil (Y4–Y6). Fly ash particles fill the pores between soil particles, enhancing the cementation effect, and assume a spherical shape that is not commonly found in nature (Y7–Y9). The addition of lime to diesel-contaminated soil further enlarges the particles cemented into clumps and reduces inter-particle pores, and the physical cementation of soil particles becomes more apparent as the diesel fuel content of the soil sample increases (Y10–Y12). Diesel fuel is more electrostatically charged under ambient conditions, and cement particles may become charged due to adsorption or ionization, forming a double layer around the particles, which tend to physically interact with diesel fuel. The increase in physical reaction products encourages particle agglomeration and fills the soil pores. When comparing the samples modified with different curing agents at the same oil content, a longitudinal comparison shows that the soil sample with lime has the smallest pores and the most obvious soil particle agglomeration, with a large number of soil particles clustered together. The soil sample with fly ash has some spherical particles linked to the soil particles, filling the pores, while the soil sample with cement still has a lumpy particle shape, but the integrity is improved with the help of the cement hydration products (Figure 11).

After summarizing the results of the Y1–Y12 tests, it was found that the use of diesel oil as a pore fluid had a significant effect on the structure of the granite residual soil. The soil underwent fragmentation and separation, changing from a flaky and blocky structure to smaller particle-sized agglomerates and fragments. The pore enlargement of the soil sample was particularly evident for the 12% oil content. A cross-sectional comparison of specimens modified with the same curing agent at different oil content rates showed that the curing agent increased the physical reaction products to promote particle agglomeration, fill the soil pores, and enhance the integrity of the soil sample. A longitudinal comparison of samples modified with different curing agents at the same oil content showed that the most significant change in the microstructure of the soil samples was caused by the curing agent fly ash, which contained particles in the form of spheres, a rare occurrence in nature.

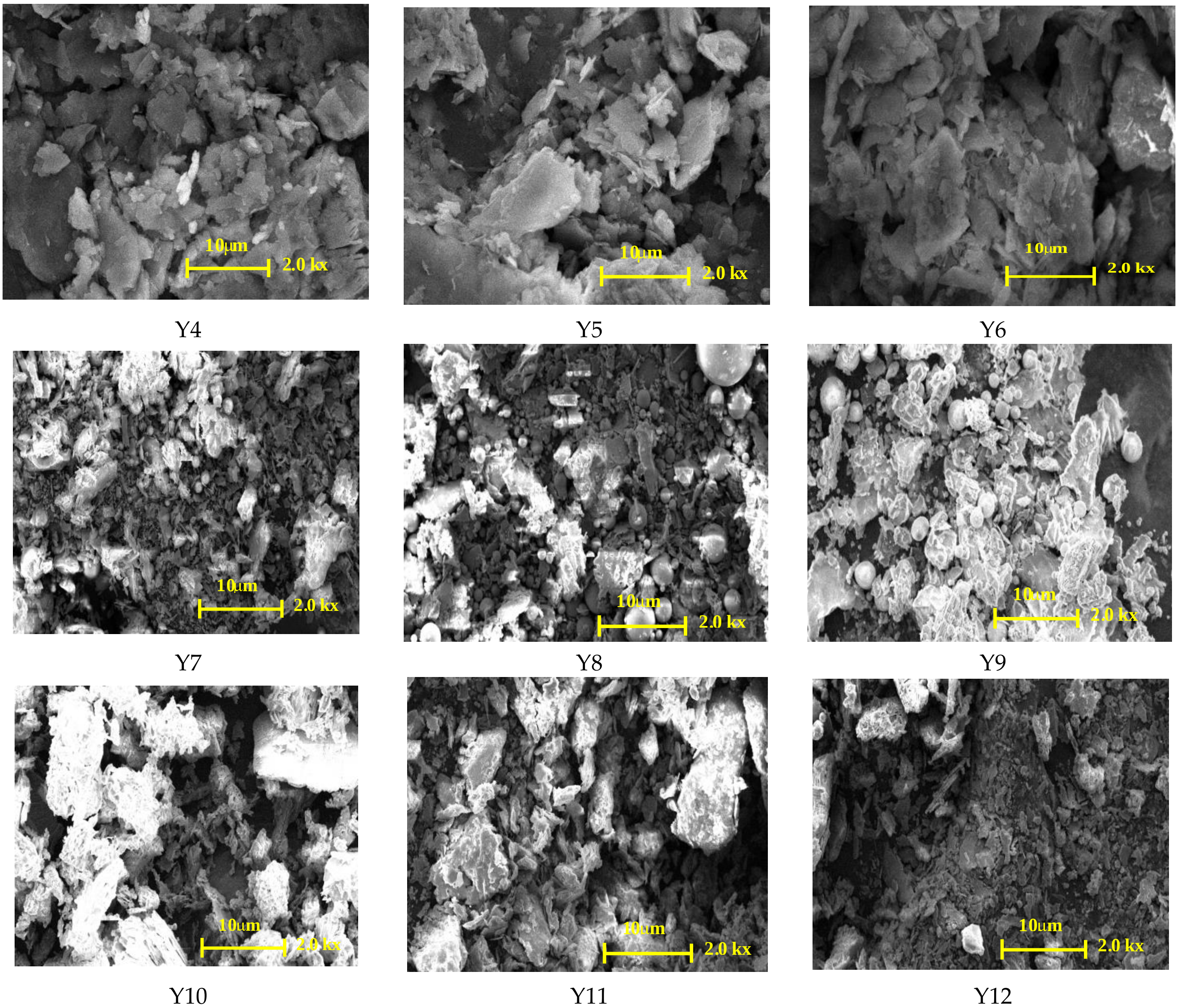

Figure 11. SEM microstructure of the modified soil.

3.4. Discussion

A similar study was conducted by Shah et al. as reported in reference [18]. The soil samples used in their research were collected from a petrochemical complex near Vadodara in Gujarat, India. The samples consisted mainly of loamy soils, with fine content ranging from 48% to 52%. In their study, the authors selected 10% of fuel-contaminated soil and found that the fuel contamination significantly weakened all soil parameters when compared to those of uncontaminated soil. Specifically, the maximum dry density decreased by approximately 4%, cohesion decreased by approximately 66%, angle of internal friction decreased by approximately 23% and unconfined compressive strength (UCS) decreased by approximately 35%. In this paper, diesel-contaminated granite residual soils with oil content ranging from 3% to 15% were chosen. The test results indicated that diesel contamination decreased all the physical and mechanical parameters of the soil, which is consistent with the findings of Shah et al. To highlight the difference before and after the improvement, the most degraded soil with 9% oil was selected for subsequent improvement studies in this paper.

Shah et al. conducted a study in which lime, fly ash, and cement were added at concentrations of 5%, 10% and 20% to 10% oil-contaminated soil. The authors measured the angle of internal friction, cohesion and unconfined compressive strength of the amended soil and found that lime was the most effective curing agent. Additionally, the authors observed that the oil content of the leachate decreased in the oil-contaminated soils with the addition of curing agents after 24 h of steady-state water infiltration. In this article, a mixture of 10% lime, 5% fly ash and 5% cement was added to the 10% oil-contaminated soil, resulting in a 371% increase in unconfined compressive strength compared to that of the oil-contaminated soil. Furthermore, the oil content of the leachate reached a minimum of 30 mg/L. In this study, cement was added at doping levels of 3%, 4%, 5% and 6%, while fly ash and lime were added at concentrations of 5%, 10%, 15% and 20%. The results of the direct shear and disintegration tests were consistent with those of Shah's study, indicating that cement, fly ash, and lime improved the internal friction angle and cohesion of the oil-contaminated soil, increased the strength and stability of the soil, and improved disintegration resistance.

At the end of their paper, Shah et al. conducted electron microscopy scanning tests on soils amended with a combination of 10% lime, 5% fly ash and 5% cement curing agents. Their results showed that the cement, fly ash and lime were capable of forming non-crystalline compounds with materials in the contaminated soil, covering the soil particles and acting as a bridge between them. In contrast, this paper analyses in greater detail how the three curing agents, cement, lime and fly ash, individually ameliorate diesel-contaminated granite residual soils, compares their variability, and explains the mechanism of curing agent amelioration. The findings of this paper are consistent with those of Shah et al. In future studies, different combinations of curing agents can be used to investigate the amelioration effect on various types of oil-contaminated soils.

4. Conclusions

Cement, fly ash and lime are regularly used curing agents for enhancing diesel-contaminated granite residual soil.

(1) The direct shear test showed that 5% cement, 15% fly ash and 6% lime were effective, with 6% lime being the most effective, resulting in a cohesive force of 122.06 kPa and an internal friction angle of 27.1°.

(2) The disintegration test showed that the 6% cement, 20% fly ash, and 10% lime admixtures had better disintegration resistance, with 10% lime being the most effective, with a disintegration time of over 650 s and a disintegration rate of 0.26181%/s.

(3) Our cross-sectional comparison of specimens modified with the same curing agent with different oil contents showed that curing agent modification promotes particle agglomeration, fills soil pores and enhances soil sample integrity.

(4) A longitudinal comparison of the samples modified with the different curing agents with the same oil content showed that fly ash had the most obvious change in soil sample microstructure while lime had the best improvement among the three curing agents.

Author Contributions: Conceptualization, Q.C.; Methodology, X.H.; Validation, Y.H.; Investigation, Z.C.; Writing–original draft, K.L. All authors have read and agreed to the published version of the manuscript.

Funding: This work is supported by the National Natural Science Foundation of China (No. 52078211. No.52279100. No. 52004328), the Natural Science Foundation of Hunan Province (2020JJ4021).

Institutional Review Board Statement: Not applicable.

Informed Consent Statement: Informed consent was obtained from all subjects involved in the study.

Data Availability Statement: Not applicable.

Conflicts of Interest: The authors declare no conflict of interest.

References

1. Zhou, X.; Huang, X.; Li, J. Reliability assessment of tunnel based on P-wave seismic velocity. *Int. J. Geomech.* **2018**, *18*, 06018030. [CrossRef]
2. Chen, Q.N.; Yang, M.; Huang, X.C. Experimental Exploration of Bearing Capacity of Clay with Multiple Inflatable Anchors. *Geofluids* **2020**, *7*, 1–11. [CrossRef]
3. Li, J.; Chen, J.; Huang, X.; Zou, G.; Deng, J. Pretreatment for Tunnel Karst Cave during Excavation: A Case Study of Guangxi, China. *Adv. Civil Eng.* **2021**, *2021*, 9013815. [CrossRef]
4. Chen, Q.; He, Y.; Zhang, Z. Effects of diesel contamination on geotechnical properties of granitic residual soil. *Arab. J. Geosci.* **2022**, *15*, 1474. [CrossRef]
5. Yang, Y.; Li, C.; Chen, Z.; Dong, Y.; Zhang, N.; Wei, Y.; Xi, H.; Wang, W. Characterization and Assessment of Organic Pollution at a Fumaric Acid Chemical Brownfield Site in Northwestern China. *Sustainability* **2022**, *14*, 12476. [CrossRef]
6. Wang, Q.; Jiang, H.Z.; Tang, D.X. Research on Granite ResiSoil and Engineering Geological Characteristics in Southern Fujian Triangle. *Fujian Geol.* **1990**, *2*, 90–99.
7. Wang, S. Remediation technology and application of contaminated sites. *Resour. Conserv. Environ. Prot.* **2022**, *252*, 90–93. [CrossRef]
8. Evgeniy, S. Study of the Processes of Electroosmotic Cleaning of Soils from Oil Pollution on a Three-dimensional Physical Model. In *E3S Web of Conferences*; EDP Sciences: Les Ulis, France, 2020; Volume 174, p. 01054.
9. Isidro, J.; López-Vizcaíno, R.; Yustres, A.; Sáez, C.; Navarro, V.; Rodrigo, M.A. Recent progress in physical and mathematical modelling of electrochemically assisted soil remediation processes. *Curr. Opin. Electrochem.* **2022**, *36*, 101115. [CrossRef]
10. Ye, C. *Research and Application of Chemical Washing Detergent for Treating Oily Soil from Jidong Oilfield*; China University of Petroleum: Beijing, China, 2020. [CrossRef]
11. Wanguang, B.; Liu, Z.; Zhang, X.; Yu, Q.; Zhang, Z. Remediation Effects of Forage Straws on the Biochemical Properties of Petroleum-contaminated Soil in the Oil Zone of Northern Shaanxi. *Acta Agrestia Sin.* **2013**, *21*, 1101–1108.
12. Yeh, X.; Wu, M.; Chen, K.; Li, W.; Yuan, J. Impacts of Bioremediation on Microbial Communities and Different Forms of Nitrogen in Petroleum Contaminated Soil. *Environ. Sci.* **2017**, *38*, 728–734. [CrossRef]
13. Wu, M.; Yuan, J.; Li, W.; Shi, Y.; Wang, X. Bioremediation of petroleum contaminated soil and activity of hydrocarbon Bioremediation of petroleum contaminated soil and activity of hydrocarbon degrading bacteria. *J. Appl. Environ. Biol.* **2016**, *22*, 878–883.
14. Wang, D.; Xu, W. Research on strength and durability of sediments solidified with high volume fly ash. *Rock Soil Mech.* **2012**, *33*, 3659–3664. [CrossRef]
15. Zeng, H.; Xu, C.; Zhou, H.; Zeng, M.; Liao, B. Effects of mixed curing agents on the remediation of soils with heavy metal pollution. *Environ. Chem.* **2012**, *31*, 1368–1374.
16. Wang, G.; Zhang, X.; Liu, X. Compression deformation characteristics and croscopic mechanism of Granite residual soil in Xiamen. *Rock Soil Mech.* **2021**, *42*, 3291–3300. [CrossRef]
17. Zeng, Z. *Study on Artificial Slope Stability in Granite*; South China University of Technology: Guangzhou, China, 2019. [CrossRef]
18. Shah, S.J.; Shroff, A.V.; Patel, J.V.; Tiwari, K.C.; Ramakrishnan, D. Stabilization of fuel oil contaminated soil—A case study. *Geotech. Geol. Eng.* **2003**, *21*, 415–427. [CrossRef]
19. Zheng, T.; Yang, J.; Liu, J. Solid properties of petroleum contaminated soil. *Hydrogeol. Eng. Geol.* **2010**, *37*, 102–106.
20. Khosravi, E.; Ghasemzadeh, H.; Sabour, M.R.; Yazdani, H. Geotechnical properties of gas oil-contaminated kaolinite. *Eng. Geol.* **2013**, *166*, 11–16. [CrossRef]
21. He, X. *Study on Properties of Diesel Contaminated Soil and Curing Effect of Cement in Changchun*; Jilin University: Changchun, China, 2015.
22. Li, M.; Meng, D.; Yao, X. Optimization of mechanical characteristics of coastal salt soil based on temperature effect. *Rock Soil Mech.* **2020**, 1–8. [CrossRef]
23. Li, Y. *Experimental Study on Disposal of Oil Pollution Soil in Sichuan-Tibet Railway*; Southwest Jiaotong University: Chengdu, China, 2019.
24. Zhang, L. *Study on the Disintegration Characteristics of Granite Residual Soil in Guangzhou*; China University of Geosciences: Wuhan, China, 2009.
25. Zhao, L. *Study on Improving Strength and DisCharacteristics of Granite Residual Soil*; Hunan University of Science and Technology: Xiangtan, China, 2015.
26. Wang, Z.; Mai, T.; Qi, C. Study on the mechanical properties and microstructural properties of compacted granite residual soil in Rong County. *Hydrogeol. Eng. Geol.* **2018**, *45*, 101–107.
27. Zhang, W.G.; Zhang, R.H.; Han, L.; Goh, A.T.C. Engineering properties of the Bukit Timah Granitic residual soil in Singapore. *Undergr. Space* **2019**, *4*, 98–108. [CrossRef]
28. Tang, L.; Xu, H.; Liu, Q. Study on Analysis of Granite. *China Highw. J.* **2022**, *35*, 75–87. Available online: http://kns.cnki.net/kcms/detail/61.1313.u.20211112.1348.002.html (accessed on 3 April 2022).
29. Meegoda, N.J.; Ratnaweera, P. Treatment of oil-contaminated soils for identification and classification. *Geotech. Test. J.* **1995**, *18*, 41–49.
30. Ratnaweera, P.; Meegoda, J. Shear strength and stress-strain behavior of contaminated soils. *Geotech Test J.* **2005**, *29*, 133–140.

31. Zhu, Y.; Li, H.; Ju, Z. Improvement of shear strength and anti-disintegration performance of compacted loess. *Coal Geol. Explor.* **2021**, *49*, 221–233.
32. Ding, Y.; Li, H.; Zhang, X.; Li, S. Using Mixture of Industrial Waste Residues and Cement to Reinforce Channel Foundation in Salinized Soils. *J. Irrig. Drain.* **2022**, *41*, 113–120. [CrossRef]
33. Semerjan, M.; Tao, S. Experimental Study on Strength Deformation and Micro-characteristics of Improved Chloride Saline Soil. *J. Yangtze River Sci. Res. Inst.* **2022**, *39*, 113–119.
34. JTG 3430-2020 Test Methods of Soils for Highway Engineering. Available online: https://www.doc88.com/p-29259489176653.html?r=1 (accessed on 28 February 2023).